

Asymptotic Giant Branch Stars in the Leo I Dwarf Spheroidal Galaxy

John W. Menzies¹, Patricia A. Whitelock^{1,2}, Michael W. Feast^{1,2}, and Noriyuki Matsunaga³

¹ *South African Astronomical Observatory, P.O.Box 9, 7935 Observatory, South Africa.*

² *Astronomy Department, University of Cape Town, 7701 Rondebosch, South Africa.*

³ *Institute of Astronomy, University of Tokyo, 2-21-1 Osawa, Mitaka, Tokyo 181-0015, Japan.*

7 June 2018

ABSTRACT

Twenty six Asymptotic Giant Branch (AGB) variables are identified in the Local Group galaxy Leo I. These include 7 Mira and 5 semi-regular variables for which periods, amplitudes and mean magnitudes are determined. The large range of periods for the Miras, $158 < P < 523$ days, suggests an AGB spanning a significant age range. The youngest must be around 1.6 Gyr while the oldest could be 10 Gyr or more. Two of these old Miras are found in the outer regions of Leo I (over 490 arcsec from the centre) where stars on the extended AGB are rare. They could provide an interesting test of third dredge-up and mass loss in old stars with low metallicity and are worth further detailed investigation. At least two stars, one a Mira, the other an irregular variable, are undergoing obscuration events due to dust ejection.

An application of the Mira period-luminosity relation to these stars yields a distance modulus for Leo I of $(m - M)_0 = 21.80 \pm 0.11$ mag (internal), ± 0.12 (total) (on a scale that puts the LMC at 18.39 mag) in good agreement with other determinations.

Key words: stars: AGB and post-AGB – stars: variables: other – galaxies: dwarf – galaxies: individual: Leo I–Local Group – galaxies:stellar content.

1 INTRODUCTION

This paper is one of a series aimed at finding and characterizing luminous Asymptotic Giant Branch variables within Local Group galaxies; it follows similar work on Phoenix and Fornax (Menzies et al. 2008; Whitelock et al. 2009). Menzies et al. (2002 hereafter Paper I) reported the discovery of several dust-enshrouded AGB stars in Leo I. Here we discuss multi-epoch JHK_S photometry of those stars which enables us to characterise them. The large-amplitude, or Mira, variables are of particular interest, first, because they tell us about the intermediate age population of which they are the most luminous representatives, secondly because they provide an independent distance calibration, via the period-luminosity (PL) relation (Whitelock et al. 2008), and thirdly because they will be major contributors to the processed material currently entering the interstellar medium of Leo I and are therefore an important source of enrichment.

Leo I is one of the most distant of the Local Group Galaxies associated with the Milky Way. It has a complex star formation history (Gallart et al. 1999; Hernandez et al. 2000; Dolphin 2002) with evidence for star formation over much of its lifetime. The most recent episode occurred

about 1 Gyr ago and may have been the result of Leo I's interaction with the Milky Way (Mateo, Olszewski & Walker 2008). Most published work indicates little evidence for population gradients (e.g. Koch et al. 2007). However, Mateo et al. (2008) find that the AGB stars are almost exclusively located within a radius of 400 arcsec whereas giant branch (GB) stars have a more extended distribution. The analysis of infrared photometry by Held et al. (2010) also indicates a strong radial gradient in the intermediate-age populations and supports the findings by Mateo et al.

Table 1: Probable AGB Stars in Leo I (excluding variable stars).

α (equinox 2000.0)	δ	L#	J	H	K_S	$J - K_S$	Memb	other name
			————— (mag) —————					
10:08:02.7	12:17:56	6010	16.00	15.29	15.04	0.96		
10:08:07.9	12:15:18	6014	16.36	15.52	15.35	1.01	m	MOW253
10:08:10.7	12:17:24	6020	16.66	15.87	15.74	0.92	m	MOW167
10:08:10.9	12:12:40	7019	16.70	15.97	15.89	0.81		
10:08:14.5	12:18:02	1024	16.07	15.27	15.07	1.00	m	MOW104
10:08:14.5	12:18:02	6011	16.10	15.28	15.08	1.02		
10:08:14.9	12:14:04	7012	15.76	15.05	14.89	0.87		
10:08:15.7	12:18:14	1069	16.70	15.98	15.80	0.90		
10:08:15.7	12:18:14	6022	16.71	16.00	15.80	0.90		
10:08:15.8	12:20:32	1098	16.40	15.66	15.48	0.93	m	MOW124
10:08:15.8	12:20:32	6026	16.42	15.65	15.47	0.95		
10:08:16.6	12:20:07	1093	16.41	15.69	15.45	0.97	m	MOW101,ALW19
10:08:17.0	12:18:15	1070	16.67	15.92	15.75	0.92	m	MOW78
10:08:17.1	12:18:52	1078	16.56	15.80	15.64	0.92	m	MOW77
10:08:17.5	12:16:15	1054	16.99	16.20	16.02	0.97	m	MOW110
10:08:18.0	12:20:09	1038	16.13	15.34	14.98	1.15		
10:08:19.4	12:17:07	1056	16.44	15.70	15.40	1.04	m	MOW67,ALW1
10:08:20.2	12:17:58	1010	15.28	14.50	14.32	0.96		
10:08:20.4	12:17:45	1061	16.97	16.20	16.02	0.95	m	MOW43
10:08:21.3	12:14:43	1016	16.00	15.21	14.96	1.05	m	MOW161
10:08:21.4	12:13:49	8023	16.38	15.61	15.37	1.01	m	MOW193
10:08:22.0	12:18:49	1030	16.25	15.48	15.32	0.94		
10:08:22.0	12:19:37	1088	16.56	15.80	15.61	0.95	m	MOW38
10:08:23.2	12:18:38	1029	16.46	15.69	15.50	0.96	m	MOW12
10:08:23.9	12:17:08	1057	16.41	15.63	15.48	0.94	m	MOW36
10:08:24.5	12:20:40	1039	16.20	15.45	15.23	0.96	m	MOW65
10:08:24.7	12:23:23	4012	16.35	15.61	15.25	1.10		
10:08:24.8	12:19:27	1033	15.71	14.92	14.58	1.14		ALW7
10:08:27.6	12:17:32	1059	16.41	15.69	15.40	1.01	m	MOW13,ALW10
10:08:27.8	12:17:55	1062	16.59	15.81	15.62	0.97	m	MOW6
10:08:28.2	12:23:30	4006	16.34	15.51	15.26	1.08		
10:08:28.3	12:20:29	1097	16.98	16.25	16.05	0.93		
10:08:28.4	12:18:49	1075	16.76	16.05	15.91	0.84	m	MOW4
10:08:28.7	12:16:25	1018	16.47	15.70	15.50	0.97	m	MOW57
10:08:29.2	12:18:32	1026	16.14	15.39	15.18	0.96	m	MOW5
10:08:29.5	12:20:43	1099	16.33	15.62	15.31	1.02		ALW13
10:08:30.0	12:16:04	1130	17.04	16.27	16.07	0.96	m	MOW85
10:08:31.0	12:17:08	1020	15.67	14.91	14.64	1.03		ALW14
10:08:31.3	12:22:48	4011	16.39	15.68	15.45	0.95		
10:08:31.5	12:18:54	1079	16.64	15.91	15.76	0.88	m	MOW25
10:08:32.5	12:18:06	1066	16.59	15.85	15.69	0.89	m	MOW30
10:08:33.6	12:15:33	1048	16.64	15.93	15.72	0.92		
10:08:33.6	12:15:41	1049	16.39	15.63	15.43	0.97	m	MOW113
10:08:33.6	12:20:11	1094	16.53	15.75	15.57	0.96		
10:08:34.4	12:15:56	1052	16.47	15.72	15.54	0.93	m	MOW107
10:08:34.9	12:19:39	1089	16.58	15.84	15.68	0.90	m	MOW66
10:08:34.9	12:21:03	1041	15.97	15.24	14.91	1.06	m	MOW109,ALW16
10:08:35.2	12:17:24	1021	16.22	15.48	15.23	0.99	m	MOW68,ALW18
10:08:36.9	12:20:11	1095	16.42	15.65	15.46	0.96	m	MOW96
10:08:37.1	12:19:24	1085	16.60	15.85	15.67	0.93	m	MOW89
10:08:38.0	12:15:52	1051	16.87	16.15	15.97	0.90	m	MOW145
10:08:38.3	12:15:45	1050	16.58	15.82	15.65	0.93	m	MOW157
10:08:39.0	12:18:32	1073	16.47	15.65	15.46	1.00		
10:08:41.8	12:20:47	1040	16.07	15.29	15.15	0.92		
10:08:42.1	12:19:32	1087	16.80	16.08	15.93	0.87	m	MOW153
10:08:42.8	12:23:45	3020	16.97	16.18	15.95	1.02	m	MOW289
10:08:44.2	12:23:46	3017	15.76	15.05	14.87	0.89		

Continued on Next Page...

α (equinox 2000.0)	δ	L#	J	H	K_S	$J - K_S$	Memb	other name
			(mag)					
10:08:44.5	12:17:23	2027	16.74	15.97	15.79	0.95	m	MOW179
10:08:45.3	12:16:32	2016	16.03	15.26	15.09	0.94		
10:08:46.0	12:22:33	3034	17.02	16.22	16.05	0.97	m	MOW279
10:08:48.3	12:19:42	2035	16.82	16.08	15.89	0.93	m	MOW236
10:08:55.5	12:14:01	9047	16.94	16.20	16.06	0.88	m	MOW324

Notes: the “other names” starting with MOW come from Mateo et al. (2008), and with ALW from Azzopardi et al. (1986). An “m” in the Memb column indicates a radial velocity member according to Mateo et al. The carbon star, ALW7, is incorrectly identified by Demers & Battinelli (2002) with their star 10.

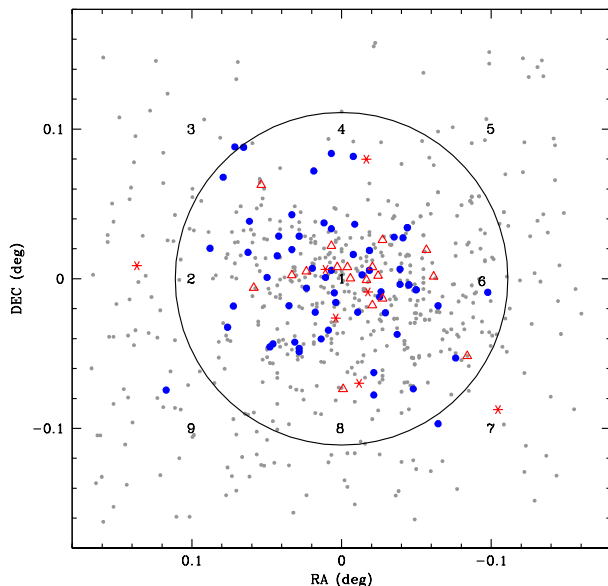


Figure 1. Positions of stars measured in Leo I. Field centres are shown by the numbers 1-9. Small grey dots are red giant branch and field stars, large dots are probable AGB stars; Miras are shown as asterisks and other variables as triangles. The circle represents a radius of 400 arcsec, within which the velocity distribution is isotropic (Mateo et al. 2008).

The chemical evolution of Leo I has been discussed by many authors, most recently by Gullieuszik et al. (2009), who use the calcium triplet to find a very narrow distribution peaking at $[M/H] = -1.2$. Very little is known about the abundances of the α -elements, but Shetrone et al. (2003) suggest that the ratio of α - to iron-peak elements is lower in dwarf spheroidals, including Leo I, than in globular clusters. If the element enrichment pattern in Leo I has been comparable to that in Fornax (Letarte 2007) then α -poor stars as old as 10 Gyr may be present, although those with ages comparable to the globular clusters will be α -rich.

Estimates for the interstellar extinction towards Leo I are low, and range from $E(B-V) = 0.01$ mag (Bellazzini et al. 2004) to $E(B-V) = 0.04$ mag (Held et al. 2001). Here we use a value of $E(B-V) = 0.04$ mag, which amounts to $A_K < 0.01$ mag and therefore has a negligible effect on anything deduced from the infrared photometry discussed here.

2 OBSERVATIONS

Observations were made with the SIRIUS camera on the Japanese-South African Infrared Survey Facility (IRSF) at SAAO, Sutherland. The camera produces simultaneous J , H and K_S images covering an approximately 7.2×7.2 arcmin square field (after dithering) with a scale of 0.45 arcsec/pixel. Initially, only two adjacent fields, one centred on the galaxy and one to the east, were observed (see Paper 1). When it was realised that there was a very red variable in the eastern field, the coverage was extended to a 3×3

grid. With generous overlaps between adjacent fields, the area observed was 19.7×19.2 arcmin squared (see Fig. 1).

Images were obtained at about 18 epochs spread over 3 years in fields 1 and 2, and between 10 and 15 epochs over about 2 years in the remaining seven fields. In each field, 10 dithered images were combined after flat-fielding and dark and sky subtraction. Typical exposures were of either 30 or 20 s for each image, depending on the seeing and on the brightness of the sky in the K_S band. Photometry was performed using DoPHOT (Schechter et al. 1993) in ‘fixed-position’ mode, using the best-seeing H -band image in each field as templates. Aladin was used to correct the coordinate system on each template and RA and Dec were determined for each measured star. This allowed a cross-correlation to be made with the 2MASS catalogue (Cutri et al. 2003), and photometric zero points were determined by comparison of our photometry with that of 2MASS. In each field, stars in common with the 2MASS catalogue with photometric quality A in each colour were identified and the IRSF zero point was adjusted to match that of 2MASS. The number of common stars per field varies from 28 in the middle field to 6 in field 4 while field 5 has only 2 stars, in common with 2MASS. The mean standard deviation over all fields of the differences between IRSF and 2MASS are 0.04 mag in J and 0.06 mag in each of H and K_S . No account was taken of possible colour transformations, such as in Kato et al. (2007). Those transformations were derived using highly reddened objects to define the red end and it is not obvious that the same transformations will apply to carbon stars.

3 COLOUR-MAGNITUDE AND COLOUR-COLOUR DIAGRAMS

Fig. 2 shows the $K_S - (J - K_S)$ diagram and Fig. 3 the $(J - H) - (H - K_S)$ diagram for all variables, which will be discussed in section 4.2, and for constant stars selected on the basis of their standard deviations: for stars with $J < 17.2$, $H < 16$ or $K_S < 16$ mag, standard deviations $\sigma < 0.1$ mag; at the faint end the limit rises to 0.2 at $J = 18.5$, and 0.25 at $H = K_S = 18.0$. Mean magnitudes from all of our observations are used in all of these plots.

The clump of points around $J - K_S \sim 1.5$ and $K_S \sim 16.6$ are most likely unresolved background galaxies (see Whitelock et al. 2009).

To illustrate the possible evolutionary state of the stars plotted, we have included two isochrones from Marigo et al. (2008) assuming a distance modulus of 21.80 and a visual extinction of $A_V = 0.12$. The first is for a 10 Gyr population with metallicity $Z = 0.001$. This has a blue-ward hook at the brightest magnitude which takes it into the region of the brightest blue stars we have selected as AGB stars ($K_S < 15$, $J - K_S \sim 0.8$); the tip of its red giant branch (TRGB) is at $K_S = 15.85$ mag. The other isochrone is for an age of 2 Gyr and $Z = 0.0012$; its TRGB is at 16.20 mag. This extends into the region occupied by the red variables, but is very uncertain beyond $J - K_S \sim 1.6$. The metallicity was chosen on the basis of the recent result of Gullieuszik et al. (2009) showing a mean $[M/H] = -1.2$ (equivalent to $Z = 0.0012$) and very little dispersion. We have not included the isochrones on the colour-colour diagram (Fig. 3) since, as we found for

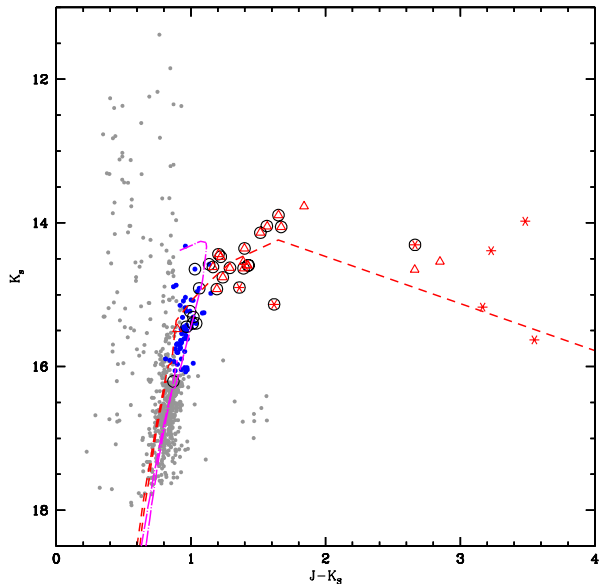


Figure 2. Colour-magnitude diagram for Leo I; Grey dots are field and red giant branch stars, asterisks are Mira variables, triangles are low amplitude, SR or Irr, variables, while large dots are other AGB stars. Carbon stars are shown as symbols surrounded by open circles. The dash-dotted and dashed curves are isochrones from Marigo et al. (2008) for populations with ages of 2 and 10 Gyr, respectively (details in text).

Fornax (Whitelock et al. 2008), there is very little correlation between the isochrones and the data points.

4 ASYMPTOTIC GIANT BRANCH

We assume that stars with $K_S < 16.1$ mag and $J - H > 0.7$ are AGB stars in Leo I; $K_S = 16.14$ mag is the TRGB (Held et al. 2010) and objects with $J - H < 0.68$ will be foreground dwarfs. In this way we make a conservative selection and can be reasonably certain that all stars selected will be AGB stars in Leo I, even if the selection also results in a few AGB stars being omitted.

From this selection we eliminated one star shown by Mateo et al. (2008) to be a radial velocity non-member. The data for the AGB stars are listed in Table 1, where the column headed L# refers to our internal star numbers, and the stars in common are noted by the Mateo et al. internal numbers prefixed by MOW. Mateo et al. assigned stars to the AGB or RGB based on the VI colour-magnitude diagram. We find two of their AGB stars fall on our RGB, both on the blue side of the RGB in our colour-magnitude diagram. A further five stars that they call RGB stars are above our dividing line, four being on the extreme red side of our AGB. There may be some physical reason for these discrepancies rather than photometric error, but this is not really relevant to the subject matter of the present paper.

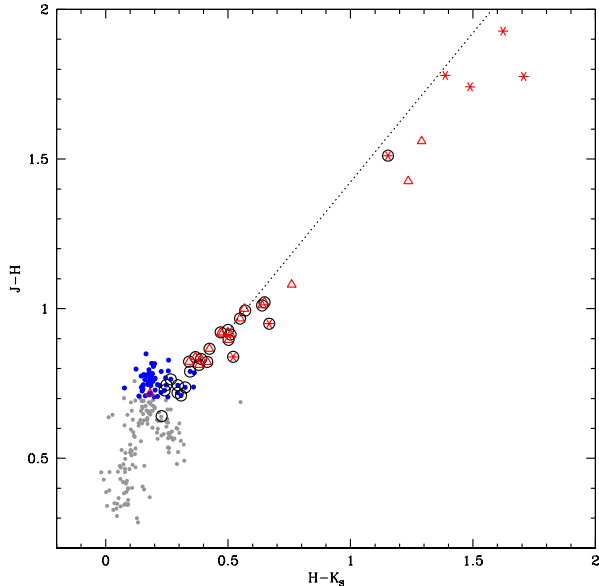


Figure 3. Two colour diagram for Leo I; symbols as in Fig. 2. The dotted line represents the locus of Galactic carbon Miras (see Whitelock et al 2009).

4.1 Carbon stars

Azzopardi, Lequeux & Westerlund (1986) and Demers & Battinelli (2002) identified 26 carbon stars in Leo I and all of these appear in our sample; they are identified in Figs. 2, 3 and in the tables. With one exception the carbon stars are all brighter than $K_S = 15.5$ ($M_K = -6.3$). In the 2 Gyr isochrone, illustrated in Fig. 2, stars brighter than $K_S = 15.7$ are carbon rich, while the 10 Gyr model does not produce C-stars at all.

The faintest carbon star, ALW12 ($K_S = 16.21$ mag), is referred to as a ‘probable carbon star’ by Azzopardi et al. (1986); its status therefore remains uncertain. If it really is carbon rich it is too faint for this enrichment to be the result of third dredge-up; it could, however, be an extrinsic carbon star (i.e. one which received its enrichment by mass transfer from a companion).

Given the low metallicity and, more importantly, the probable low oxygen abundance (Shetrone et al. 2003) of Leo I we would anticipate that all of the intermediate-age AGB variable stars will be carbon-rich. It is less obvious what we should expect for very old AGB variables, but we do not expect to see high mass-loss, i.e. very red, stars that are oxygen-rich in this environment (Lagadec & Zijlstra 2008).

The Miras L7020 and L2077 are outside the regions surveyed for carbon stars. The other three periodic variables that have no carbon star identification have $J - K_S > 2.6$ (L6015 is different and is discussed in the next section); presumably all these stars are extremely faint at short wavelengths.

Held et al. (2010) do a detailed division of AGB stars into presumed oxygen- and carbon-rich on the basis of their colours and compare carbon star numbers to theoretical predictions.

Table 2. Periodic Red Variables.

L#	P (day)	J	ΔJ	H	ΔH	K_S	ΔK_S	$J - K_S$	m_{bol}	Sp	2MASS	other names
					(mag)							
Miras												
1019	158	16.75	1.21	15.80	0.89	15.14	0.62	1.61	18.58	C	10082751+1216539	ALW9
8026	180	16.30	0.78	15.40	0.61	14.91	0.41	1.39	18.23	C	10082387+1214165	ALW4
7020	191	18.34	1.87	16.56	1.57	15.17	1.24	3.17	18.20		10080111+1213144	
4005	252	16.97	0.55	15.46	0.53	14.31	0.48	2.66	17.62	C	10082268+1223159	C13
2077	283	19.18	1.87	17.25	1.23	15.63	1.17	3.53	18.33			E
1077	336	17.62	1.23	15.88	1.01	14.39	0.81	3.23	17.32		10082927+1218516	A
1064	523	17.46	1.52	15.68	1.29	13.98	1.03	3.48	16.63		10082225+1217571	C
SRs												
6015	141	16.38	0.29	15.66	0.34	15.48	0.26	0.90			10080593+1215228	MOW273
1031	216	16.01	0.29	15.09	0.19	14.59	0.21	1.42	17.92	C	10082561+1218571	C10
1043	222	16.02	0.40	15.10	0.25	14.63	0.19	1.39	17.94	C	10083988+1222144	C08
1037	316	15.73	0.60	14.70	0.35	14.06	0.21	1.67	17.50	C	10082008+1220023	C02
1067	999	17.31	0.43	15.89	0.31	14.65	0.29	2.66	17.92		10084120+1218068	D, MOW128

Notes: ABCDE sources identified in Paper I. ALW numbers from Azzopardi, Lequeux & Westerlund (1986). C numbers from Demers & Battinelli (2002). MOW numbers from Mateo et al. (2008).

Table 3. Variables without measured periods.

L#	J	δJ	H	δH	K_S	δK_S	$J - K_S$	m_{bol}	Sp	2MASS	other names
					(mag)						
1080	17.39	2.3	15.83	1.1	14.54	0.9	2.85	17.73		10082730+1218571	B
1012	15.54	0.3	14.53	0.3	13.89	0.3	1.65	17.33	C	10082064+1218364	C03
1013	15.65	0.4	14.69	0.2	14.14	0.3	1.52	17.52	C	10083233+1218460	C07
1014	15.61	0.4	14.53	0.3	13.77	0.3	1.84	17.25		10082170+1218575	
1025	15.75	0.2	14.86	0.2	14.36	0.2	1.40	17.68	C	10082528+1218301	ALW8,C06
1035	16.02	0.6	15.10	0.4	14.59	0.3	1.42	17.93	C	10081288+1219379	C11
6006	15.61	0.2	14.61	0.1	14.04	0.1	1.56	17.44	C	10081170+1218334	C04
1022	15.91	0.3	15.05	0.2	14.62	0.2	1.29		C	10082175+1217249	ALW3,C09
8024	16.12	0.3	15.30	0.2	14.92	0.2	1.19		C	10082634+1214026	ALW6
6012	15.93	0.3	15.02	0.2	14.54	0.2	1.39	17.85		10081288+1219379	
1036	16.00	0.3	15.17	0.2	14.76	0.2	1.24		C	10082849+1218485	ALW11,C12
1011	15.69	0.2	14.86	0.1	14.47	0.1	1.22		C	10082254+1218259	ALW5,C05
1023	15.64	0.3	14.80	0.2	14.44	0.2	1.20		C	10081995+1217414	ALW2,C01
1028	15.78	0.3	14.96	0.2	14.61	0.2	1.16		C	10083471+1218374	ALW15

Notes: other names follow the same convention as Table 2.

4.2 Variable stars

We examined all of the bright red stars ($J - K_S > 1.0$) with significant standard deviations ($\sigma_{JHK_S} \geq 0.1$ mag) for periodic variations. (Although it is bluer than this limit, L6015, with $J - K_S = 0.9$, is relatively bright and was recognised as a variable when its photometry was noticed to have much larger standard deviations in all wavebands than stars of similar brightness.)

Table 2 lists the Fourier mean JHK_S magnitudes for the periodic variables, the peak-to-peak amplitudes (ΔJ , ΔH , ΔK_S), mean $J - K_S$, and apparent bolometric magnitude, m_{bol} ; a C indicates it is a known carbon star, while 2MASS and other identifications are also given.

Following Whitelock et al. (2006) we call variables with $\Delta K_S > 0.4$ mag Miras, and lower amplitude variables semi-regulars (SRs). Figs. 4 and 5 illustrate the light curves of the Mira and SR variables, respectively, phased at their best-fitting periods. Note that the periods of the Miras are, in general, much more secure than those of the SR variables.

With the exception of L4005 the Miras are all definite Miras. L4005 is included with the group because of its large amplitude, but its light curve is not well defined so its status as a Mira is uncertain. L8026 is almost certainly a Mira variable, but its light curve is not well defined as only 8 H observations (7 K_S) were available to define its period and mean magnitude and they do not cover maximum light. L2077 is clearly a Mira, but also has a long-term trend, it is discussed in Section 4.3.

Stars which are clearly variable, but for which we have been unable to establish a period, are listed in Table 3 together with the full range of their variations: δJ , δH , δK_S . Some of these will be irregular variables, others are SRs, but require more observations to define their periods.

The variables are identified on the colour-magnitude (Fig. 2) and $(J - H) - (H - K_S)$ (Fig. 3) diagrams. The reddest stars (those with $J - K_S \geq 1.1$) are all variable. It is generally understood that AGB stars move to the right and down in Fig. 2 and to the upper right in Fig. 3 as their

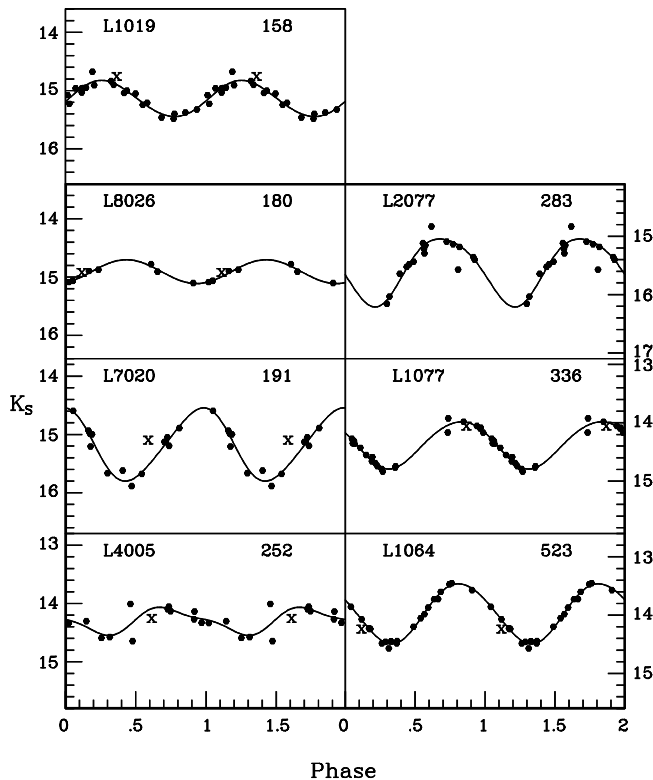


Figure 4. The K_S light curves for the Mira variables; each point is plotted twice to emphasize the periodicity and the curves are the best-fitting second-order sine curves (first order for L8026). The X shows the 2MASS observation. The period in days is shown in the top right corner of each panel.

mass-loss increases and their shells become optically thick at JHK_S .

The SR variable L6015, at $J - K_S \sim 0.9$ is significantly less red than any of the other variables, which indicates that it has a very low mass-loss rate. Nevertheless, the period established here puts it on the same $PL(K)$ relation (see section 4.4) as the Miras and suggests that it is pulsating in the fundamental mode (Wood 2000). This star is a radial velocity member of Leo I according to Mateo et al. (2008).

4.3 Long term trends

Whitelock et al. (2006) established that among Galactic carbon-variables about one third of Miras showed obscuration events, as did an unknown fraction of non-Mira variables. An obscuration event is generally associated with the ejection of a puff of dust into our line of sight, and the phenomenon is particularly well illustrated by the light-curve of II Lup (Feast et al. 2003) which covers a time span of 18 years. The ejection of puffs of dust in random directions is well studied among the hydrogen-deficient R CrB (RCB) stars.

Fig. 6 illustrates two of the Leo I variables that show obvious long-term trends. L1080 is clearly variable, but not periodic. Its light-curve is reminiscent of that of an RCB star, in that it shows SR-type variability before going into a deep minimum. Its colours are very red for a non-Mira and

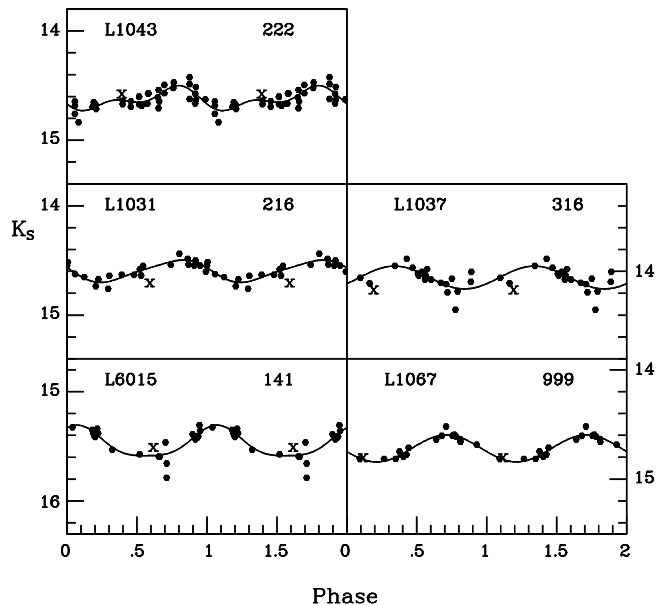


Figure 5. The K_S light curves for the SR variables; see Fig. 4 for details.

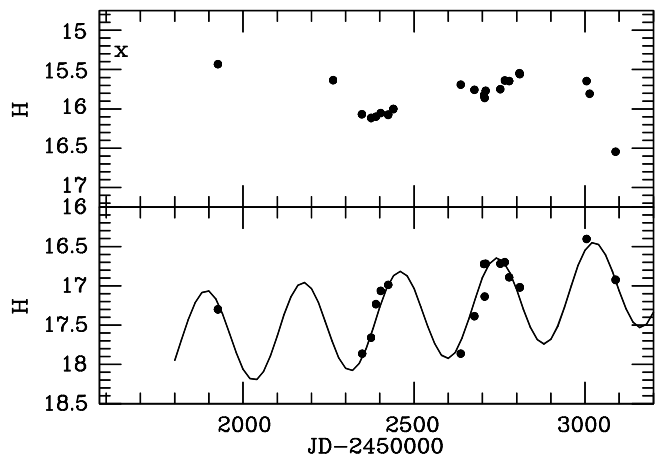


Figure 6. The H light curves for L1080 (top) and L2077 (bottom) are shown as a function of Julian Date (JD). For L2077 the fitted curve is a 280 day sine function plus a long term trend represented as a 10000 day sine function; note that the mean light level brightens by more than 0.5 mag over 5 cycles. L1080 shows large variations, but no clear periodicity; X indicates the 2MASS measurement.

in the colour-magnitude diagram (Fig. 2) it is found among the extreme AGB stars with $J - K_S > 2.5$.

L2077 is a Mira with a clear period of 280 days, but its mean magnitude also brightened by over 0.5 mag at H (by about 1.0 mag at J and 0.5 mag at K_S) during the 3 years we monitored it. It is rather faint for its period as is discussed in section 4.5.

Most of the observations by Held et al. (2010) for the variables are completely consistent with the values in Tables 2 and 3, the one exception being the SR variable L1037 (21484 in their table 5), which we both identify with C02 from Demers & Battinelli (2002). They find $J = 17.12$, $H = 15.74$, $K = 14.83$, which is much redder than the values in Table 2 and the 2MASS observation and, as well, is outside

of the range illustrated in Fig. 5. The Held et al. observations were made almost a year after ours and may indicate the ejection of a dust shell.

Whitelock et al. (2009) identified several variables in Fornax that seemed to show examples of dust shell ejecta.

4.4 Distribution of AGB stars and variables

In Fig 1 we show where the AGB stars and variables lie with respect to the centre of Leo I. As found by Mateo et al. (2008), we see that most of the AGB stars lie within a circle of radius 400 arcsec and are less widely distributed than the RGB stars. Mateo et al. convincingly demonstrate that the extended AGB cannot be from the same population as the bulk of the GB stars.

It is perhaps surprising that two of the Mira variables, L2077 and L7020, lie well outside the 400 arcsec circle (they are 490.4 and 493.4 arcsec from the centre, respectively). There are only three probable AGB stars lying outside the circle, one of them being a confirmed radial velocity member. It is possible that these two Miras, which have relatively short periods, and, by analogy, the other three with short periods, are old stars and not from the same population as the main extended AGB. This is discussed further in section 6.

4.5 Bolometric magnitudes and the period-luminosity (PL) relation

In calculating the bolometric magnitudes of the variables we assume $E(B-V) = 0.04$ mag, but note that the difference in distance modulus derived from this assumption and $E(B-V) = 0.00$ mag is less than 0.01 mag.

Fig. 7 shows the PL(K) relation for the periodic variables in Leo I compared to the relation for C-rich Miras in the LMC:

$$M_K = -3.51[\log P - 2.38] - 7.24, \quad (1)$$

from Whitelock, Feast & van Leeuwen (2008) on the assumption that the distance modulus of Leo I is 21.80 (see below). Five of the Miras fall close to the relation and the other two considerably below it. As these stars are red compared to the LMC objects used to define the PL relation, this is hardly surprising and we would anticipate that they are affected by circumstellar extinction at K .

Apparent bolometric magnitudes were calculated from colour dependent bolometric corrections, as was done in our previous work on Fornax (Whitelock et al. 2009). To determine the distance to Leo I we fit the following equation to the Mira observations:

$$M_{bol} = -4.271 - 3.31[\log P - 2.5] \quad (2)$$

(This is A1 from Whitelock et al. (2009), and assumes an LMC modulus of 18.39.) Using all 7 Miras we obtain $(m - M) = 21.80 \pm 0.11$ mag (internal error only). Eliminating L4005 (which has an uncertain status as a Mira) and using the other 6 stars gives $(m - M) = 21.84 \pm 0.12$ mag. Eliminating L2077 (which was undergoing an obscuration event when we observed it, see section 4.3) and using the other 6 stars gives $(m - M) = 21.69 \pm 0.04$ mag. Fig. 8 shows the PL relation with all the variables and the relation just derived for all 7 Miras.

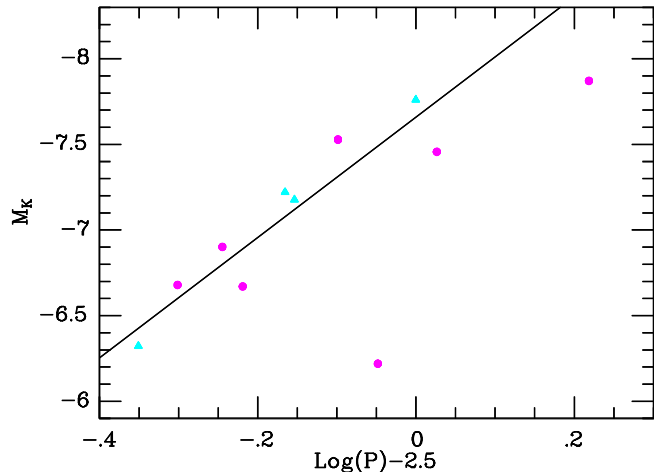


Figure 7. The M_K PL relation for the periodic variables in Leo I on the assumption that the distance modulus is 21.80 mag; Miras are shown as circles and SRs as triangles. The line is the K PL relation derived from C-rich LMC Miras.

Note that the SR variable L6015 does not appear in Fig. 8; we cannot use the same method to estimate its bolometric magnitude because the bolometric corrections are not defined for stars with $J - K < 1.4$ (on the SAAO system).

Table 3 includes estimates of the bolometric magnitudes for the variables without periods where their colours allow it to be estimated, but these should be used with caution as we do not know that these variables are comparable to those for which the bolometric correction was established.

To establish the complete (external plus internal) error on the distance modulus we must include the uncertainty of the adopted distance modulus for the LMC, 18.39 ± 0.05 (van Leeuwen et al. 2007, derived from Cepheid variables). Taking this into account the distance modulus of Leo I from all seven Miras is, $(m - M)_0 = 21.80 \pm 0.12$.

Omitting L2077, on the assumption that its apparent low luminosity results from obscuration by a non-uniform shell, results in a modulus of $(m - M)_0 = 21.69 \pm 0.06$. However, in view of the selection process involved, we have increased the error in this case by adding in quadrature the, primarily intrinsic, rms scatter per star. Whitelock et al. (2008) found the scatter for LMC Miras about the PL to be ± 0.12 mag, so we estimate the rms scatter per star for the 6 stars here as $0.12/\sqrt{6} = 0.049$. This increases the standard error from 0.06 to 0.08.

5 THE DISTANCE TO LEO I

Here we compare the distance obtained above with independent estimates from the literature using RR Lyrae variables (RRs) and the tip of the red giant branch. These are expressed in a self consistent way, assuming the interstellar reddening amounts to $E(B - V) = 0.04$ mag (which affects estimates based on shorter wavelength measurements although its impact on our infrared measures is minimal). The results are given in Table 4.

Held et al. (2001) discuss B and V photometry for RRs they discovered in Leo I. Assuming $E(B - V) = 0.04$ mag for the galaxy, they find a mean value for the RRs of $V_0 =$

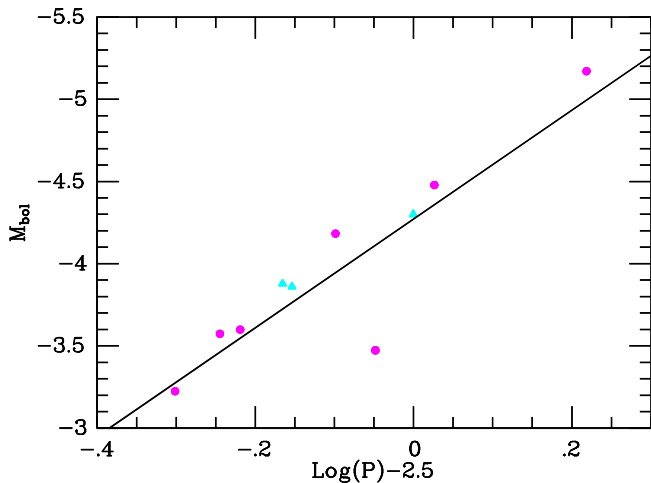


Figure 8. The bolometric PL relation for the periodic variables in Leo I. Miras are shown as circles and SRs as triangles. The line is the result of fitting equation A1 from Whitelock et al. (2009) to all 6 Miras, which gives a distance modulus of 21.80 mag.

Table 4. Distance to Leo I.

method	$(m - M)_0$ (mag)	reference
RRs	21.88 ± 0.14	Held et al. (2001) revised
	21.79 ± 0.14	see text
TRGB(<i>J</i>)	21.97 ± 0.13	Bellazzini (2004) revised
TRGB(<i>JHK</i>)	21.88 ± 0.13	Held et al. (2010) revised
Miras	21.80 ± 0.12	this paper

22.48 ± 0.12 . We assume the following expression for the absolute magnitude of the RRs (Feast 2010):

$$M_V = 0.21([\text{Fe}/\text{H}] + 1.5) + 0.68 (\pm 0.10), \quad (3)$$

which was derived from a mean of the trigonometrical, pulsation and statistical parallaxes. Held et al. adopted $[\text{Fe}/\text{H}] = -1.82$, giving $M_V = +0.61$. Hence $(m - M)_0 = 22.48 - 0.61 = 21.87 \pm 0.14$ (standard error from Held et al.). Equation 3, with the mean $[\text{Fe}/\text{H}]$ value for the LMC from Gratton et al. (2004), gives a distance modulus for the LMC of 18.38 mag. Thus, on a scale of $(m - M)_0 = 18.39$ for the LMC, the RRs give $(m - M)_0 = 21.88 \pm 0.14$ for Leo I.

However, Gullieuszik et al. (2009) recently determined the metallicity of Leo I as $[\text{M}/\text{H}] = -1.2$, with a very narrow intrinsic dispersion of only ± 0.08 . Converting this to $[\text{Fe}/\text{H}]$ depends on the metallicity scale and is rather uncertain, but using the globular cluster comparison made by Gullieuszik et al., we would estimate this corresponds to $[\text{Fe}/\text{H}] \sim -1.4$. Following the same argument as above this leads to $M_V = 0.70$ for the RRs and $(m - M)_0 = 21.79 \pm 0.14$ mag for the distance modulus.

Bellazzini et al. (2004) discuss the distance to Leo I from the TRGB, using an independent calibration of M_I^{TRGB} based on adopted distances of ω Cen and 47 Tuc. They find $I(\text{TRGB}) = 17.97$. Assuming $E(B - V) = 0.01$ mag and $[\text{M}/\text{H}] \sim -1.2$ they obtain $(m - M)_0 = 22.02 \pm 0.13$. With our adopted value of $E(B - V) = 0.04$ mag, this becomes $(m - M)_0 = 21.97 \pm 0.13$. Held et al. (2010) derive a modulus

of 22.04 ± 0.11 from the TRGB at *JHK* after applying population corrections. As in the case of Fornax discussed by Whitelock et al. (2009) their basic scale is 0.16 mag longer than that adopted here. Thus on a scale consistent with the other results in Table 4 the infrared TRGB distance is 21.88. Note, however, Salaris & Girardi (2005) have urged caution in using the TRGB as a distance indicator in the presence of a significant intermediate mass population — a situation that obviously applies to Leo I.

Each method of distance determination has its own uncertainties, and although touched upon here the details of these are beyond the scope of this paper. Within those uncertainties the various distance estimates to Leo I agree remarkably well and the Miras provide a useful estimate of the distance, independent of the more commonly used methods. If the metallicity of the C-Miras in Leo I is lower than that in the LMC (which seems likely) this result indicates that there are no large metallicity effects in the Mira PL relation.

6 DISCUSSION

Our most direct information about the ages and masses of carbon Miras comes from those discovered in Magellanic Cloud clusters by Nishida et al. (2000). These have periods of between 450 and 526 days and follow the same bolometric PL relation as the carbon-rich field Miras (Whitelock et al. 2003). The clusters in which they are found have ages of about 1.6 Gyr (Mucciarelli et al. 2007a; Mucciarelli, Origlia & Ferraro 2007b; Glatt et al. 2008) and we would therefore suggest that the longest period Mira in Leo I, L1064 with $P=523$ days, is of similar age.

The other Miras must be older; how much older is difficult to quantify. In view of the fact that two of the stars with $P < 300$ days are found in the outer part of Leo I (section 4.4) it is tempting to suggest that they may be much older, possibly comparable to the 10 Gyr or more that is thought to be characteristic of the RGB stars. Note that in the Galaxy oxygen-rich Miras with $P < 300$ days are found in relatively metal-rich ($[\text{Fe}/\text{H}] > -1$) globular clusters, which have ages greater than 10 Gyr. Within these clusters, their periods and therefore of course their magnitudes are proportional to the metallicity of the parent cluster (Feast, Whitelock & Menzies 2002). Miras are not found in the more metal-deficient clusters.

Although we have yet to confirm spectroscopically that these two Miras are carbon-rich, their colours certainly suggest it. Most models do not produce carbon stars or high-mass-loss objects at ages of 10 Gyr, although recent work suggests it might happen. Karakas (2010) modelled a $1M_\odot$ star with $Z=0.0001$ and found that it experienced 26 thermal pulses and a small amount of third-dredge-up. In an envelope with such a low metallicity, even a small amount of dredge-up was enough to make $\text{C}/\text{O} > 1$ and produce a carbon star. This is clearly an area where more work is needed and these stars are worth a more detailed investigation.

For the future, with the next generation of large telescopes working in the infrared, Mira variables will prove vital distance indicators for studying populations of old and intermediate age stars, where they will be amongst the most

luminous objects, easily identified via their large amplitude variations.

ACKNOWLEDGMENTS

We are grateful to the following colleagues for acquiring images for this programme: Toshihiko Tanabé, Takahiro Naoi, Shogo Nishiyama, Yoshifusa Ita and Barbara Cunow.

This research has made use of Aladin. This publication makes use of data products from the Two Micron All Sky Survey, which is a joint project of the University of Massachusetts and the Infrared Processing and Analysis Center/California Institute of Technology, funded by the National Aeronautics and Space Administration and the National Science Foundation. This material is based upon work supported financially by the South African National Research Foundation. We also thank Enrico Held for sending us his 2010 paper in advance of publication.

REFERENCES

- Azzopardi M., Lequeux J., Westerlund B. E., 1986, *A&A*, 161 232
- Bellazzini M., Gennari N., Ferraro, F. R., Sollima A., 2004, *MNRAS*, 354, 708
- Cutri R. M., et al., 2003, University of Massachusetts and Infrared Processing and Analysis Center (IPAC/California Institute of Technology), 2MASS
- Dolphin A. E., 2002, *MNRAS*, 332, 91
- Demers S., Battinelli P., 2002, *AJ*, 123, 238
- Feast M. W., 2010, in: (eds.) C. Sterken, N. Samus and L. Szabados, “Variable stars, the Galactic halo and galaxy formation”, in press, 2009arXiv0912.4159
- Feast M. W., Whitelock P. A., Menzies J. W., *MNRAS*, 2002, 329, L7
- Feast M. W., Whitelock P. A., Marang F., *MNRAS*, 2003, 346, 878
- Gallart C., Freedman W. L., Aparicio A., Bertelli, G., Chiosi C., 1999, *AJ*, 118, 2245
- Glatt K. et al., 2008, *AJ*, 136, 1703
- Gratton R. G., Bragaglia A., Clementini G., Carretta E., Di Fabrizio L., Maio M., Taribello E., 2004, *A&A*, 421, 937
- Gullieuszik M., Held E. V., Saviane I., Rizzi L., 2009, *A&A*, 500, 735
- Held E. V., Clementini G., Rizzi L., Momany Y., 2001, *ApJ*, 562, L39
- Held E. V., Gullieuszik M., Rizzi L., Girardi L., Marigo P., Saviane I., 2010, *MNRAS* in press
- Hernandez X., Gilmore G., Valls-Gabaud D., 2000, *MNRAS*, 317, 831
- Karakas A. I., 2010, *MNRAS*, in press, arXiv:0912.2142
- Kato D., et al., 2007, *PASJ*, 59, 615
- Koch A., Wilkinson M. I., Kleyna J. T., Gilmore G. F., Grebel E. K., Mackey A. D., Evans N. W., Wyse R. F. G., 2007, *ApJ*, 657, 241
- Lagadec E., Zijlstra A. A., 2008, *MNRAS*, 390, L59
- Letarte B., 2007, Thesis, University of Groningen
- Marigo P., Girardi L., Bressan A., Groenewegen M. A. T., Silva L., Granato G. L., 2008, *A&A*, 482, 883
- Mateo M., Olszewski E. W., Walker M. G., 2008, *ApJ*, 675, 201
- Menzies J., Feast M., Tanabé T., Whitelock P., Nakada Y., 2002, *MNRAS*, 335, 923 (Paper I)
- Menzies J., Feast M., Whitelock P., Olivier E., Matsunaga N., da Costa G., 2008, *MNRAS*, 385, 1045
- Mucciarelli A., Ferraro F. R., Origlia L., Fusi Pecci F., 2007a, *AJ*, 133, 2053
- Mucciarelli A., Origlia L., Ferraro F. R., 2007b, *AJ*, 134, 1813
- Nishida S., Tanabé T., Nakada Y., Matsumoto S., Sekiguchi K., Glass I.S., 2003, *MNRAS*, 313, 136
- Salaris M., Girardi L., 2005, *MNRAS*, 357 669
- Schechter P. L., Mateo M., Saha A., 1993, *PASP*, 105, 1342
- Shetrone M., Venn K. A., Tolstoy E., Primas F., Hill V., Kaufer A., 2003, *AJ*, 125, 684
- van Leeuwen F., Feast M. W., Whitelock P. A., Laney C. D., 2007, *MNRAS*, 379, 723
- Whitelock P. A., Feast M. W., van Loon J. Th., Zijlstra A. A., 2003, *MNRAS*, 342, 86
- Whitelock P. A., Feast M. W., Marang F., Groenewegen M. A. T., 2006 *MNRAS* 369, 751
- Whitelock P. A., Feast M. W., van Leeuwen F., 2008, *MNRAS*, 386, 313
- Whitelock P. A., Menzies J. W., Feast M. W., Matsunaga N., Tanabé T., Ita Y., 2009, *MNRAS*, 394, 795
- Wood P., 2000, *Publ. Astron. Soc. Aust.*, 17, 18